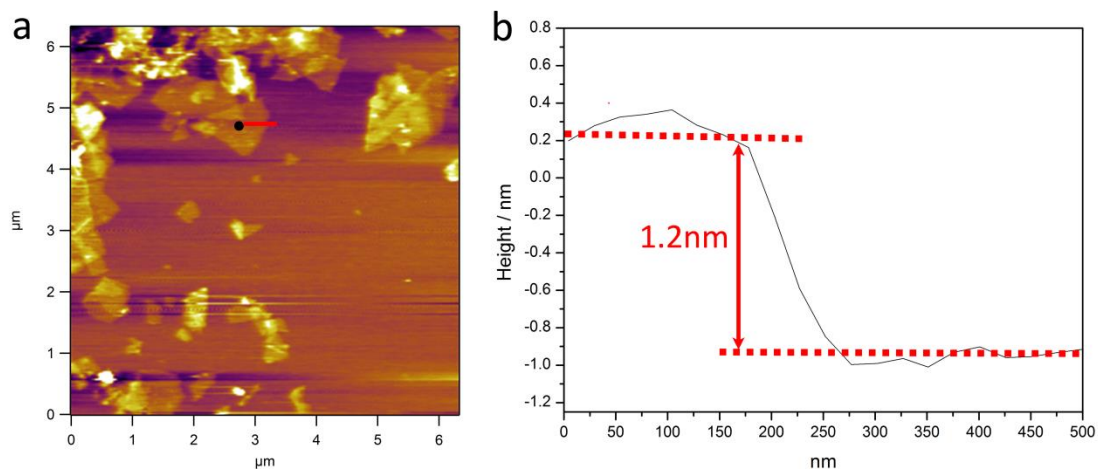
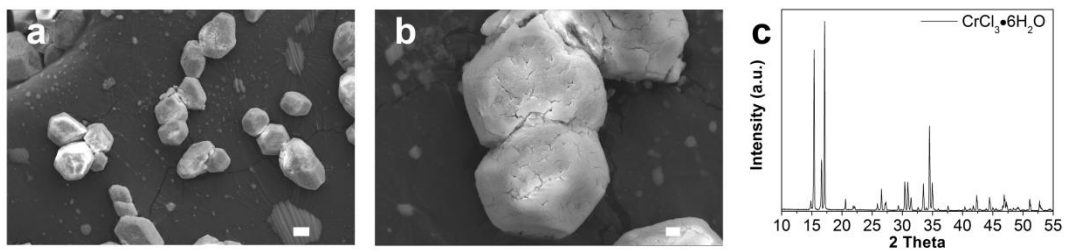


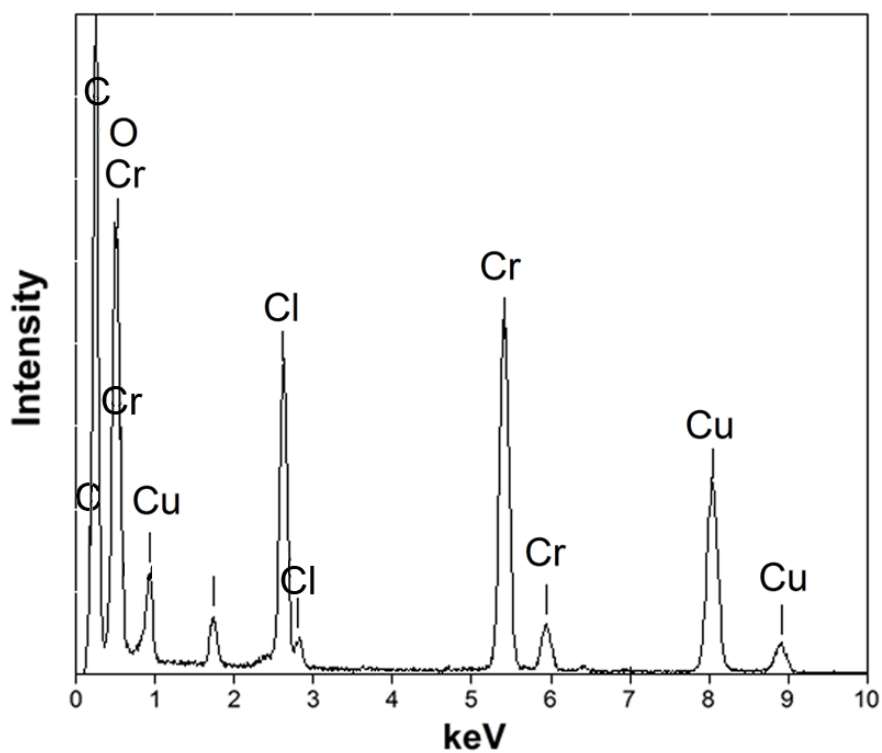
**Supplementary Figure 1 | SEM of the vermiculite samples.** Vermiculite (a) before and (b) after heat treatment. Scale bars, 100  $\mu\text{m}$  (a) and 500  $\mu\text{m}$  (b).



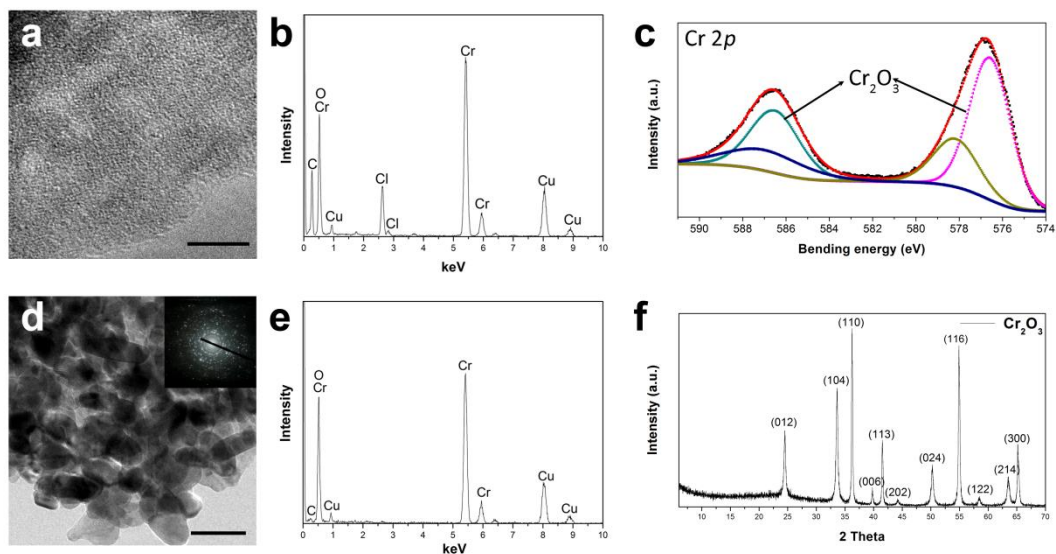
**Supplementary Figure 2 | Thickness of Cr<sub>2</sub>O<sub>3</sub> nanosheet measured by AFM.** AFM image of the Cr<sub>2</sub>O<sub>3</sub> obtained by alcohol lamp heating (a), (b) Height profile along the red line indicated in (a), which is consistent with a sheet thickness of 1.2 nm.



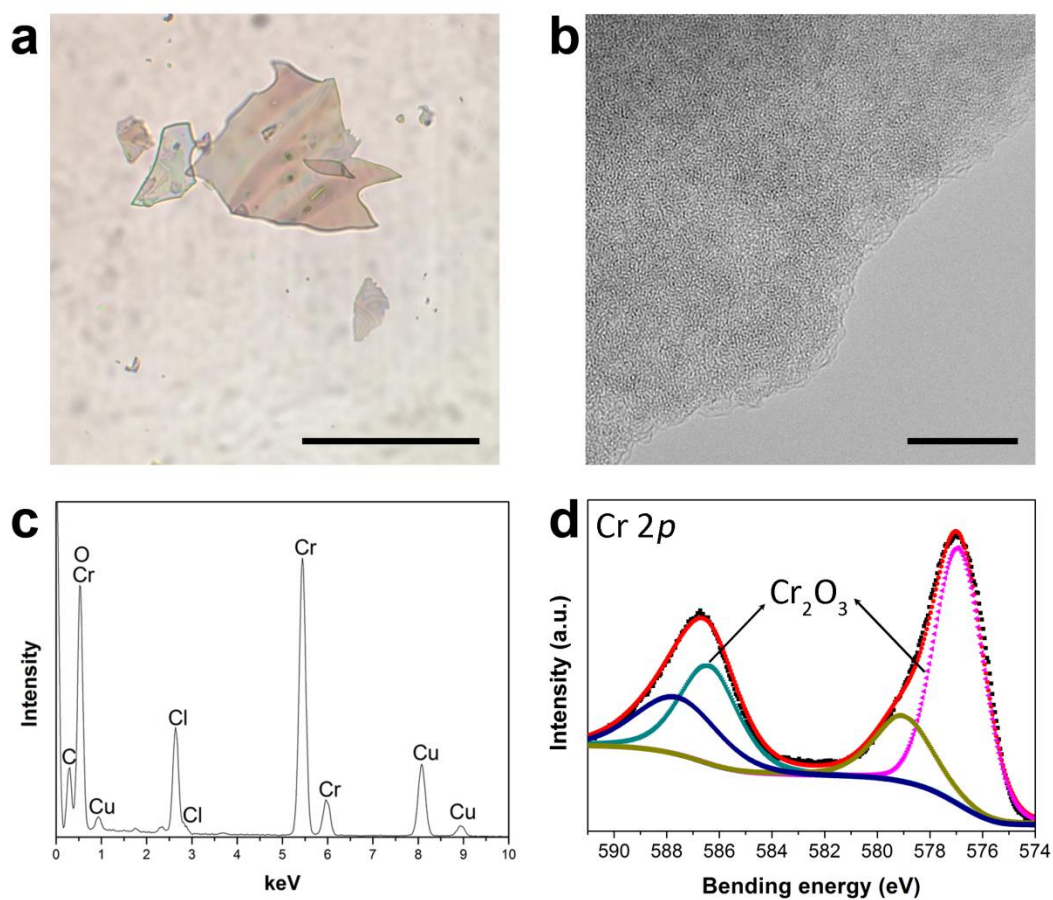
**Supplementary Figure 3 | Characterization of  $\text{CrCl}_3 \cdot 6\text{H}_2\text{O}$  starting material. (a,b)** SEM images and (c) XRD pattern of the  $\text{CrCl}_3 \cdot 6\text{H}_2\text{O}$  raw material. Scale bar, 10  $\mu\text{m}$  (a) and 2  $\mu\text{m}$  (b).



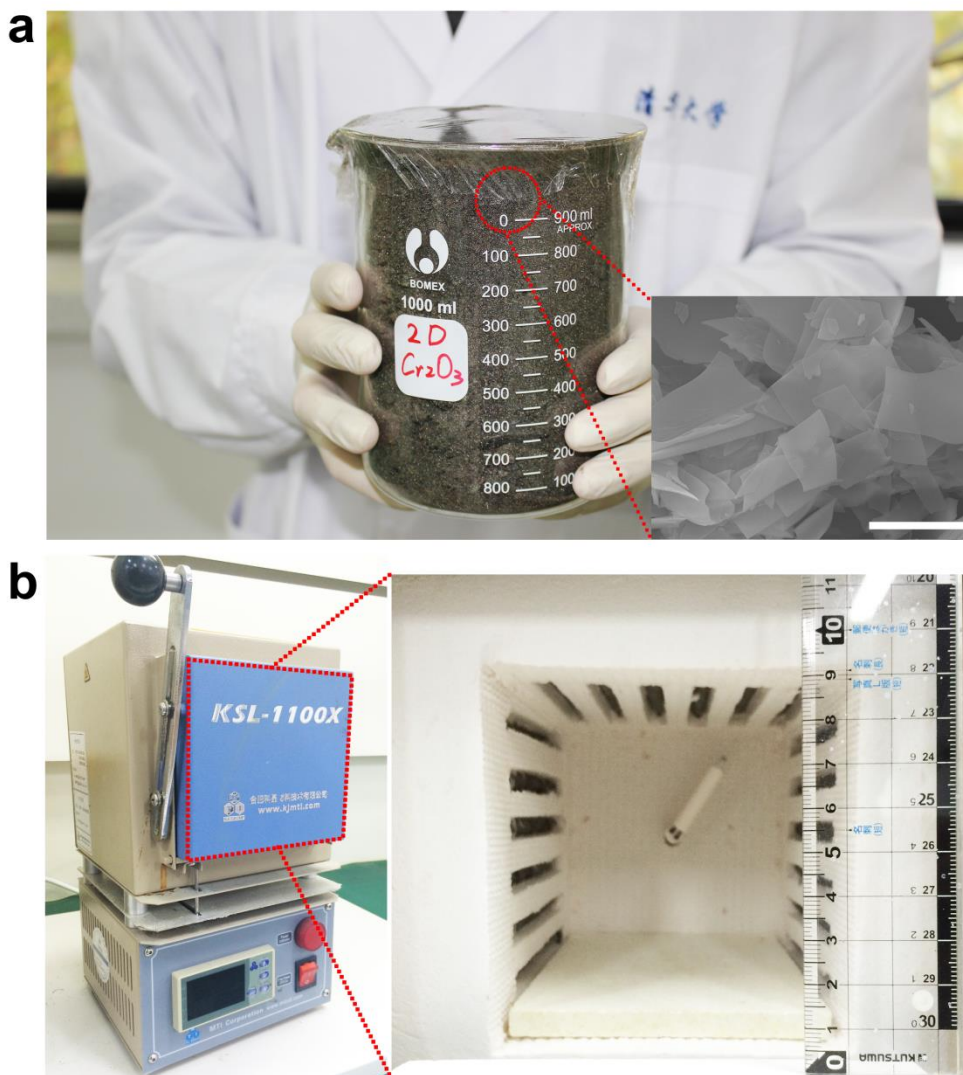
**Supplementary Figure 4 | EDS of material produced by microwave heating.** EDS analysis results suggested the sample is CrOCl (obtained by heating  $\text{CrCl}_3 \cdot 6\text{H}_2\text{O}$  in a microwave oven).



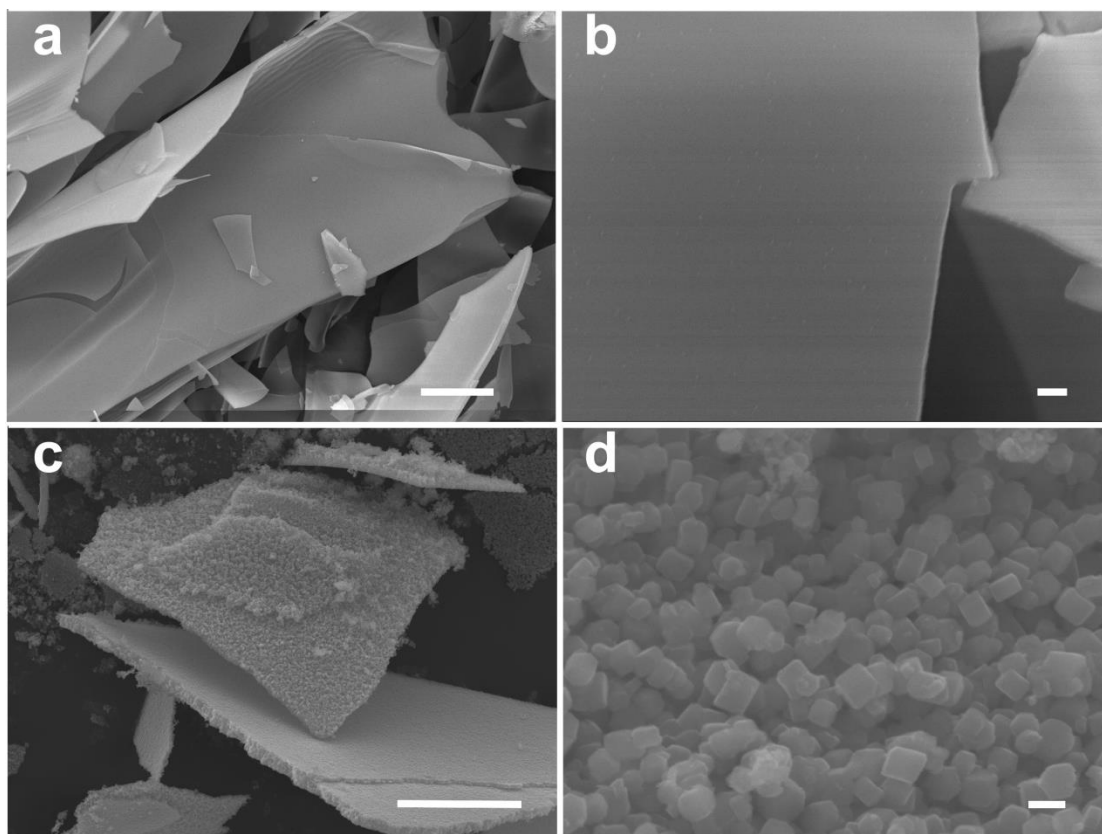
**Supplementary Figure 5 | Characterization of  $\text{Cr}_2\text{O}_3$ .** The  $\text{Cr}_2\text{O}_3$  was obtained by heating  $\text{CrCl}_3 \cdot 6\text{H}_2\text{O}$  using an alcohol lamp. **(a)** HRTEM image of the  $\text{Cr}_2\text{O}_3$  nanosheets. **(b)** EDS result for the samples shown in **(a)**. **(c)** XPS results of the  $\text{Cr}_2\text{O}_3$ . **(d)** TEM image of a sheet formed by  $\text{Cr}_2\text{O}_3$  crystal particles (Inset) Corresponding electron diffraction pattern. **(e)** EDS result for the  $\text{Cr}_2\text{O}_3$  shown in **(d)**. **(f)** XRD pattern of the  $\text{Cr}_2\text{O}_3$  sample. Scale bar, 5 nm **(a)** and 100 nm **(d)**.



**Supplementary Figure 6 | Characterization of  $\text{Cr}_2\text{O}_3$ .** The  $\text{Cr}_2\text{O}_3$  was obtained by heating  $\text{CrCl}_3 \cdot 6\text{H}_2\text{O}$  using the muffle furnace. **(a)** Optical microscopy image of  $\text{Cr}_2\text{O}_3$ . **(b)** HRTEM image of  $\text{Cr}_2\text{O}_3$  nanosheets. **(c)** EDS result for the  $\text{Cr}_2\text{O}_3$ . **(d)** XPS result of the  $\text{Cr}_2\text{O}_3$ . Scale bar, 50  $\mu\text{m}$  **(a)** and 10 nm **(b)**.

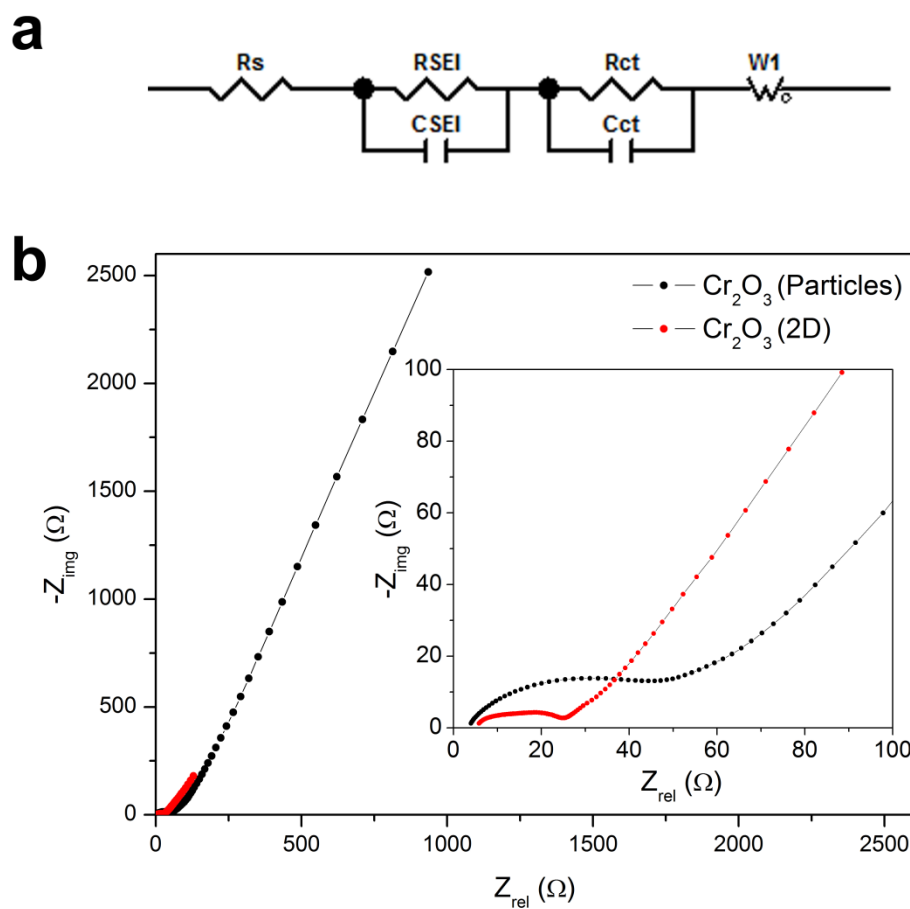


**Supplementary Figure 7 | Large-scale production.** (a) 1000 ml batch of 2D chromium oxide nanosheets. (Inset) SEM image of the chromium oxide nanosheets. Scale bar, 10  $\mu\text{m}$ . (b) The muffle furnace used in the experiments. The interior dimensions of the furnace are approximately  $10 \times 10 \times 10 \text{ cm}^3$ .

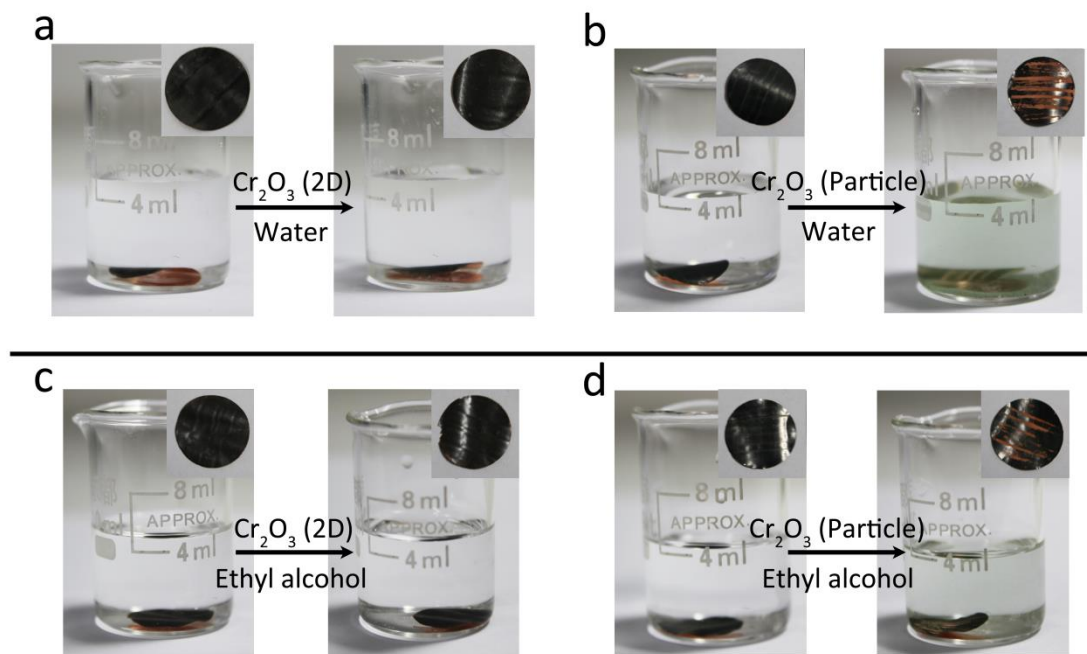


**Supplementary Figure 8 | SEM images of  $\text{Cr}_2\text{O}_3$ .** (a,b) The  $\text{Cr}_2\text{O}_3$  obtained by heating  $\text{CrCl}_3 \cdot 6\text{H}_2\text{O}$  in a muffle furnace at  $400\text{ }^\circ\text{C}$  for 15 minutes without a temperature-ramping period. (c,d) The  $\text{Cr}_2\text{O}_3$  obtained by heating  $\text{CrCl}_3 \cdot 6\text{H}_2\text{O}$  in a muffle furnace at  $400\text{ }^\circ\text{C}$  for 15 minutes with a temperature ramp rate of  $5\text{ }^\circ\text{C}/\text{min}$ . Scale bar,  $10\text{ }\mu\text{m}$  (a,c) and  $200\text{ nm}$  (b,d).



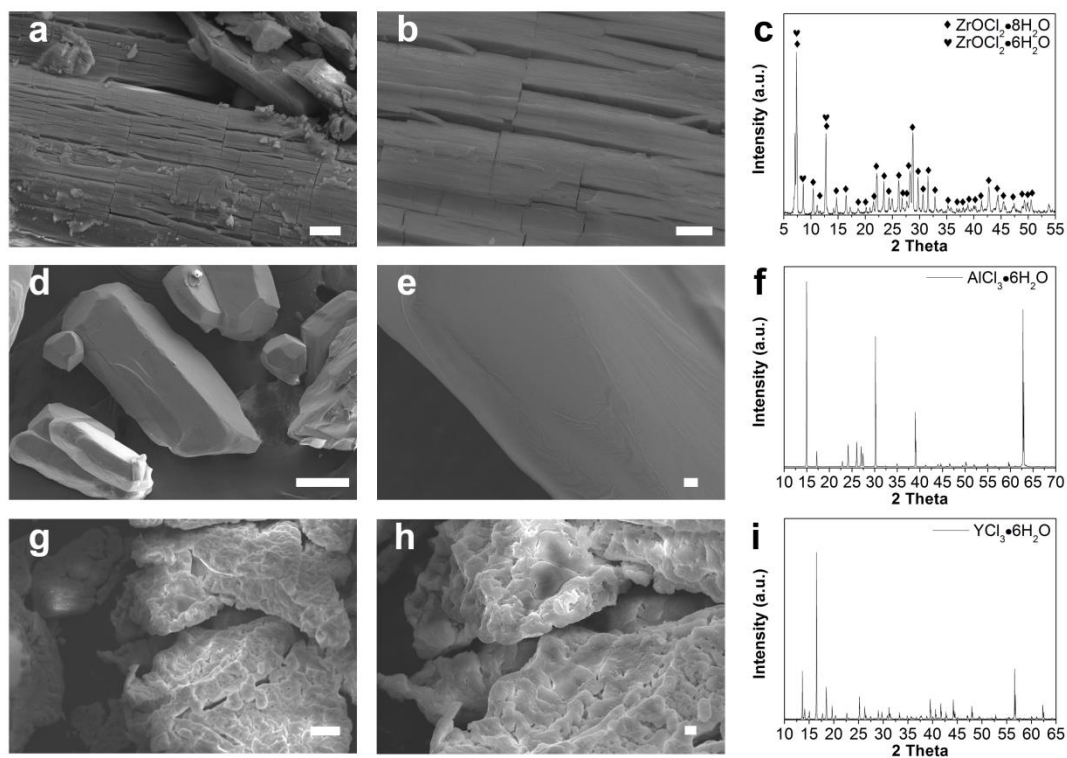


**Supplementary Figure 9 | The impedance of the electrodes.** (a) Equivalent circuit used for fitting the impedance spectra of the electrodes. (b) Nyquist plots of EIS spectra of the graphene/ $\text{Cr}_2\text{O}_3$  (2D) electrodes and graphene/  $\text{Cr}_2\text{O}_3$  (particle)/PVDF electrodes in delithiation stage.

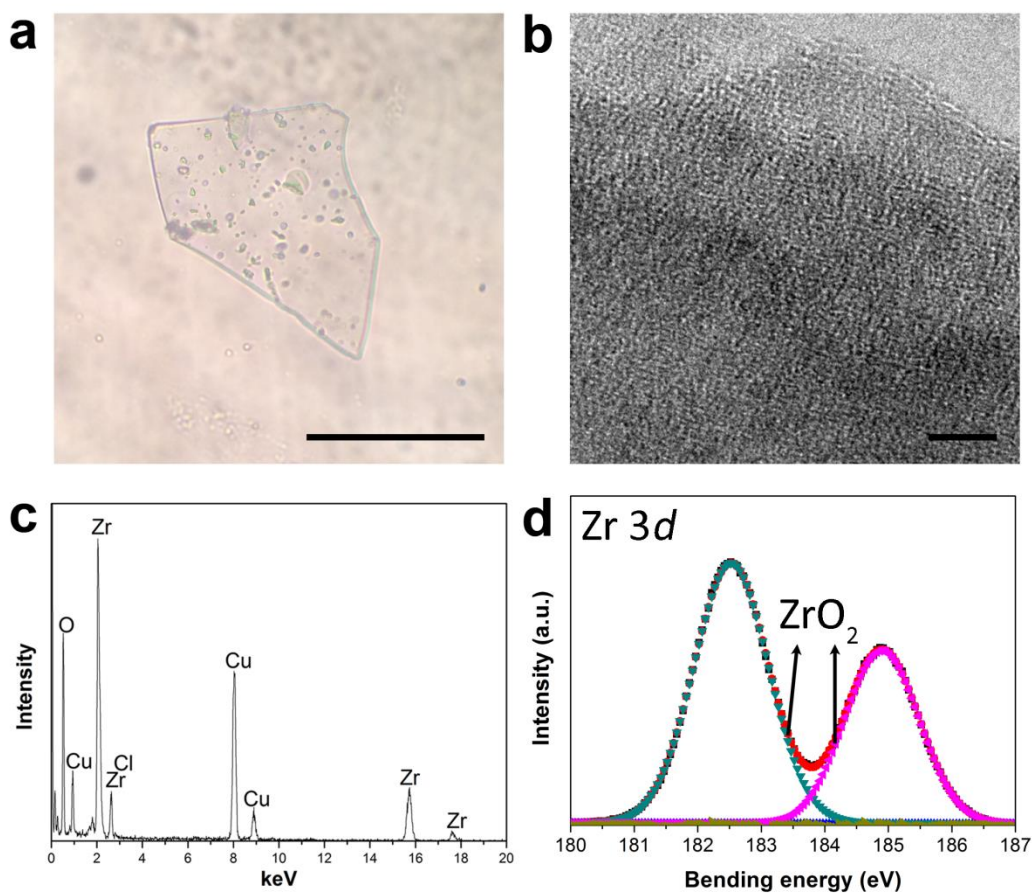


**Supplementary Figure 10 | Adhesion performance of  $\text{Cr}_2\text{O}_3$  (2D and particles).**

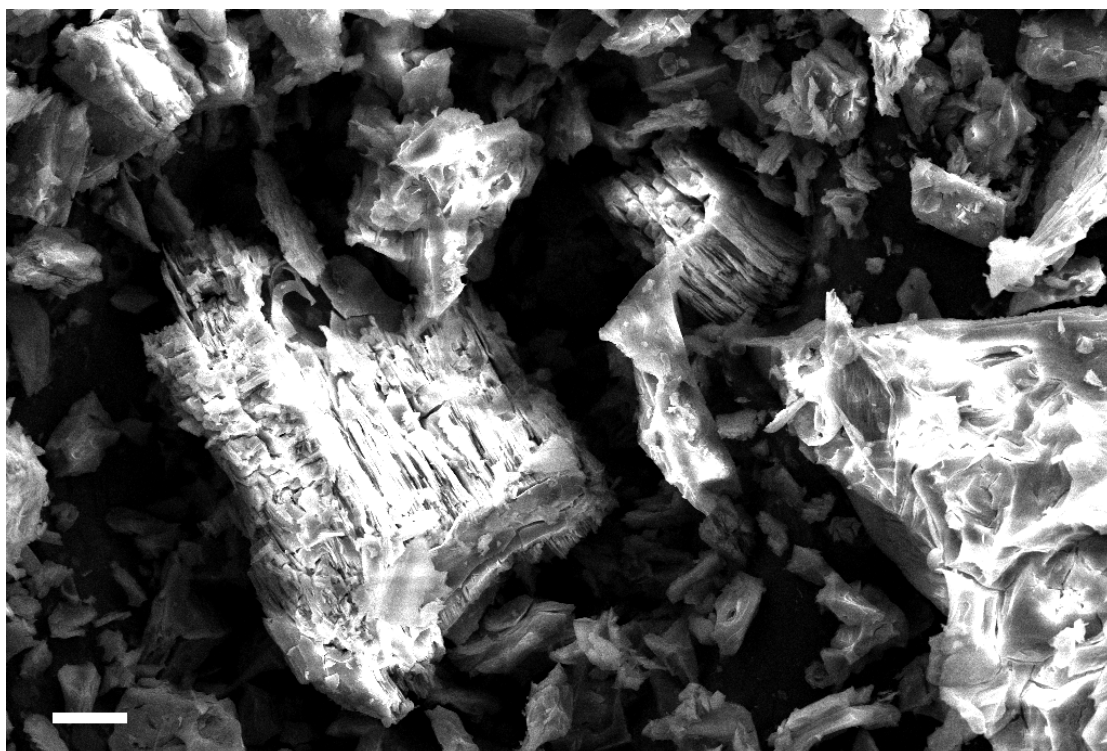
The 2D  $\text{Cr}_2\text{O}_3$ /graphene layers showed strong adhesion to the current collector (copper foil) as well as between layers. Panels (a) and (b) show the (a)  $\text{Cr}_2\text{O}_3$  (2D)/graphene electrode and (b)  $\text{Cr}_2\text{O}_3$  (particle)/graphene/PVDF electrode before (left of panel) and after (right of panel) they were ultrasonically cleaned in water for 5 minutes. Panels (c) and (d) show the  $\text{Cr}_2\text{O}_3$  (2D)/graphene electrode and  $\text{Cr}_2\text{O}_3$  (particle)/graphene/PVDF electrode before (left of panel) and after (right of panel) they were ultrasonically cleaned in ethyl alcohol for five minutes. The  $\text{Cr}_2\text{O}_3$  (2D)/graphene electrode remained intact after being ultrasonically cleaned in water or ethyl alcohol. However, the  $\text{Cr}_2\text{O}_3$  (particle)/graphene/PVDF electrode separated from the copper foil after ultrasonication.



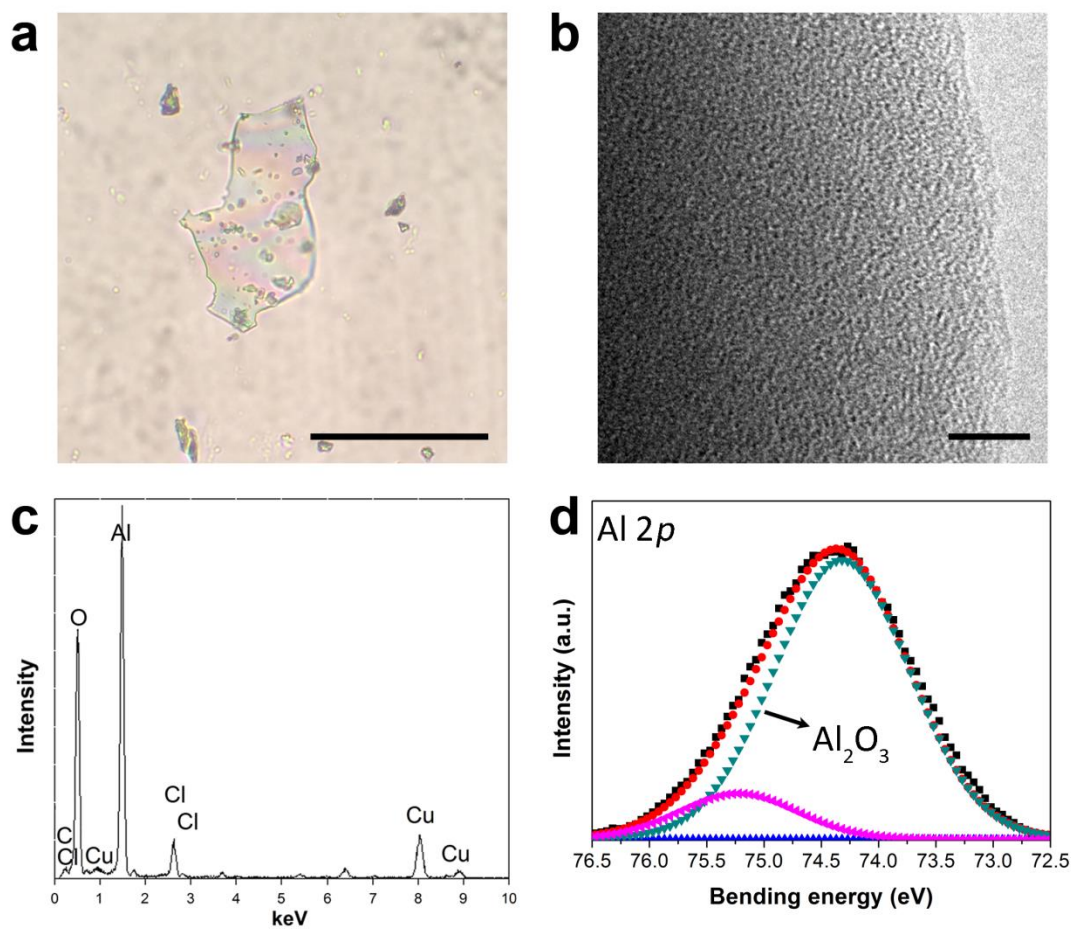
**Supplementary Figure 11 | Characterization of raw materials.** (a,b) SEM images and (c) XRD pattern of the  $\text{ZrOCl}_2 \cdot 8\text{H}_2\text{O}$  raw material including few  $\text{ZrOCl}_2 \cdot 6\text{H}_2\text{O}$ . (d,e) SEM images and (f) XRD pattern of the  $\text{AlCl}_3 \cdot 6\text{H}_2\text{O}$  raw material. (g,h) SEM images and (i) XRD pattern of the  $\text{YCl}_3 \cdot 6\text{H}_2\text{O}$  raw material. Scale bar  $10\ \mu\text{m}$  (a,g),  $2\ \mu\text{m}$  (b,e,h) and  $100\ \mu\text{m}$  (d).



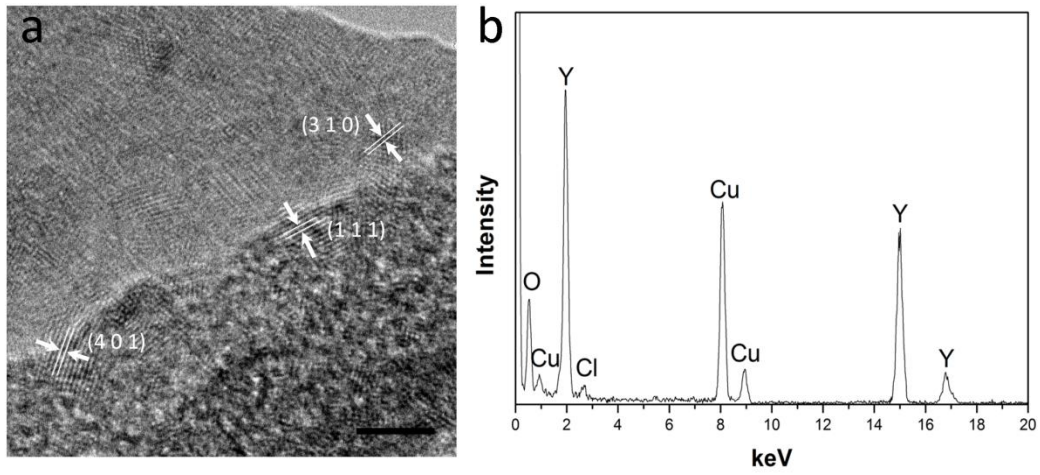
**Supplementary Figure 12 | Characterization of ZrO<sub>2</sub>.** ZrO<sub>2</sub> was obtained by heating ZrOCl<sub>2</sub>·8H<sub>2</sub>O using a microwave oven. (a) Optical microscopy images of ZrO<sub>2</sub>. (b) HRTEM image of ZrO<sub>2</sub> nanosheets. (c) EDS result for the ZrO<sub>2</sub>. (d) XPS result of the ZrO<sub>2</sub>. Scale bar, 50  $\mu$ m (a) and 5 nm (b).



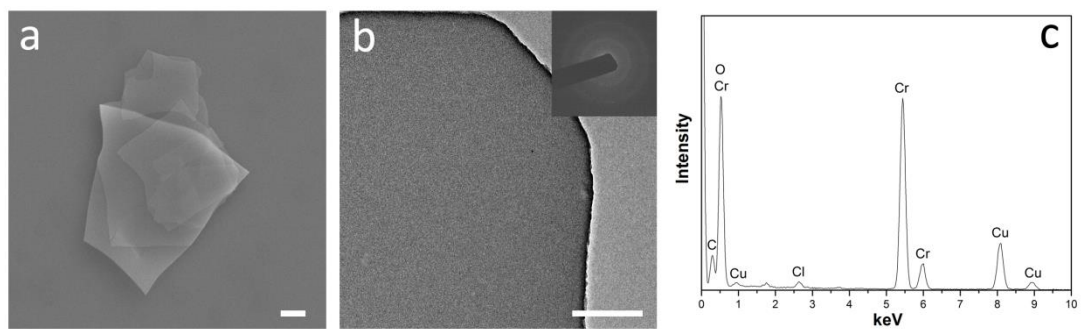
**Supplementary Figure 13 | SEM image of the Al<sub>2</sub>O<sub>3</sub>.** Al<sub>2</sub>O<sub>3</sub> obtained by heating the AlCl<sub>3</sub>·6H<sub>2</sub>O crystals in a glass bottle for approximately five minutes using an alcohol lamp. Scale bar, 20 μm.



**Supplementary Figure 14 | Characterization of Al<sub>2</sub>O<sub>3</sub>.** Al<sub>2</sub>O<sub>3</sub> was obtained by heating AlCl<sub>3</sub>·6H<sub>2</sub>O using a heating gun. (a) Optical microscopy images of Al<sub>2</sub>O<sub>3</sub>. (b) HRTEM image of Al<sub>2</sub>O<sub>3</sub> nanosheets. (c) EDS result for the Al<sub>2</sub>O<sub>3</sub>. (d) XPS result of the Al<sub>2</sub>O<sub>3</sub>. Scale bar, 50 μm (a) and 10 nm (b).

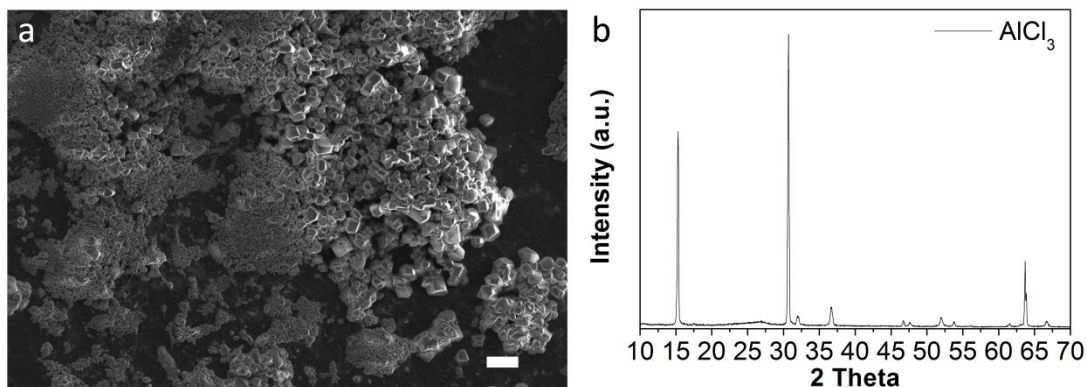


**Supplementary Figure 15 | Characterization of  $\text{Y}_2\text{O}_3$ .** (a) HRTEM image of  $\text{Y}_2\text{O}_3$  nanosheets. (b) EDS result for the  $\text{Y}_2\text{O}_3$ . Scale bar, 5 nm (a).

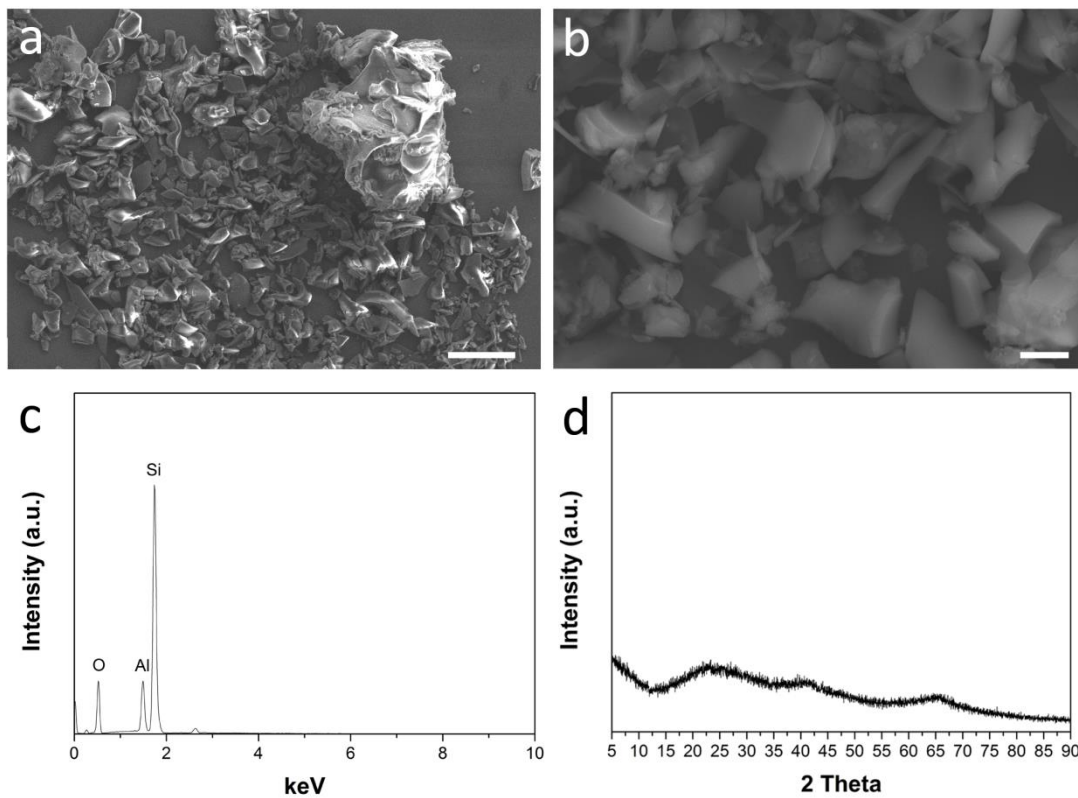


**Supplementary Figure 16 | Characterization of the  $\text{Cr}_2\text{O}_3$ .**  $\text{Cr}_2\text{O}_3$  was obtained using a rapid thermal oven. (a) SEM (b) TEM (the inset is corresponding electron diffraction pattern) and (c) EDS results. Scale bar, 2  $\mu\text{m}$  (a) and 200 nm (b).





**Supplementary Figure 17 | The products fabricated from anhydrous AlCl<sub>3</sub>.** (a) SEM image and (b) XRD pattern of the products fabricated from anhydrous AlCl<sub>3</sub> by rapid heating process (heated the anhydrous AlCl<sub>3</sub> using the alcohol lamp). Scale bar, 10  $\mu\text{m}$ . During the heating process, the AlCl<sub>3</sub> was volatilized without chemical reaction. Accordingly, XRD unmodified anhydrous AlCl<sub>3</sub> after treatment. The obtained product was composed of micron-sized particles without 2D structure.



**Supplementary Figure 18 | The products fabricated from  $\text{AlNO}_3 \cdot 9\text{H}_2\text{O}$ . (a,b)** SEM images, (c) EDS result and (d) XRD pattern of the products fabricated from  $\text{AlNO}_3 \cdot 9\text{H}_2\text{O}$  by rapid heating (heated for approximately five minutes using alcohol lamp). According to the XRD, EDS and SEM results, the obtained amorphous aluminum oxide was micron-sized particles without obvious 2D structure. Scale bar, 10  $\mu\text{m}$  (a) and 2  $\mu\text{m}$  (b).